# INDUSTRIALLY FEASIBLE REAR SIDE CONCEPT FOR n-TYPE SILICON SOLAR CELLS APPROACHING 700 mV OF $V_{OC}$

D.Suwito, U.Jäger, J.Benick, S. Janz, M.Hermle, R.Preu, S.W.Glunz

Fraunhofer Institute for Solar Energy Systems ISE, Heidenhofstr. 2, D-79110 Freiburg
Corresponding author: Dominik Suwito, Tel.: +49-761-4588-5435, Fax.: +49-761-4588-9250,
E-mail: dominik.suwito@ise.fraunhofer.de

ABSTRACT: n-Type silicon as base material offers a great potential for highly efficient solar cells. In this work we present an industrially feasible approach for the rear passivation and contacting of n-type cells on the basis of phosphorous doped amorphous silicon carbide in combination with a laser process (*PassDop*). The *PassDop* layer deposited by plasma enhanced chemical vapor deposition (PECVD) fulfills three requirements at the same time: (i) The recombination at the passivated surface is reduced to surface recombination velocities (SRV) as low as 3 cm/s. (ii) The layer acts as a dopant source during a laser process yielding local back surface fields (LBSF) underneath the metal contact points reducing the SRV at the very contact area to below 3000 cm/s. (iii) The *PassDop* layer in combination with evaporated aluminium results in an effective rear reflectance of 93±1 % of the cells including the metallization points. On low temperature high-efficiency n-type solar cell structures this approach proved to be extremely reproducible and led to efficiencies of up to 22.4 % ($V_{oc}$=701 mV, *FF*=80.1 %).

Keywords: c-Si, n-type solar cells, amorphous silicon carbide, laser doping

## 1 INTRODUCTION

Highest solar cell performances in the industrial production are achieved on n-type silicon. Sunpower and Sanyo report on efficiencies well above 20 % [1, 2], however on demanding cell structures. Very high conversion efficiencies have also been reported for laboratory scale n-type PERL (passivated emitter, rear locally diffused) solar cells by Benick *et al.* [3, 4]. These cells feature an $Al_2O_3$ passivated front side boron emitter and a PECVD (plasma enhanced chemical vapor deposited) $SiN_x$ or a thermally grown $SiO_2$ passivation on the rear side of the cell. An additional local $n^+$ diffusion ($R_{sheet}$≈20 Ohm/sq) underneath the rear side point contacts results in a further reduction of the rear minority carrier recombination. With this structure the contribution of the base to the total saturation current density of the cell can be reduced to below 40 fA/cm$^2$. However, this high-efficiency approach for the rear side comprises an additional diffusion step as well as photolithography, both stating major obstacles for an industrial implementation. This work is dedicated to overcome the time consuming processes on the rear side of this cell type by developing an efficient rear side passivation and contacting scheme on the basis of industrial feasible PECVD and laser processes. The approach results in a PERC (passivated emitter and rear cell) structure with a local $n^+$ BSF induced by laser doping from a phosphorous doped amorphous silicon carbide layer. In the following this novel approach will be referred to as *PassDop* process.

## 2 EXPERIMENTAL DETAILS

### 2.1 Lifetime samples

In a first experiment we aimed at establishing the doping efficiency of our passivation layer during laser exposure. Here the parameter of major importance is the effectiveness of the laser induced high-low junction in terms of a reduction of the recombination rate at the laser points. For accessing this quantity n-Fz 1 Ωcm silicon wafers were bifacially passivated by phosphorous doped amorphous silicon carbide. The layers were deposited by PECVD in an AK400M reactor from Roth&Rau featuring a high frequency (13.65 MHz) generator as well as a microwave antenna (2.45 GHz) using silane ($SiH_4$) and methane ($CH_4$) as process gases. The doping of the amorphous matrix was realized by adding phosphine ($PH_3$) to the precursor gases. The minority carrier lifetimes $\tau_{eff}$ were evaluated by means of the QSS-PC (quasi steady state photoconductance) technique [5] at an injection level of $\Delta n$=5×10$^{14}$ cm$^{-3}$ before and after the symmetric application of a laser process to both sides of the samples. The IR laser (1030 nm) used in this experiment was a Rofin Starcut Disc 100 ICQ disk laser exhibiting a pulse length of 1 µs and an array of laser points with $L_p$=1 mm spacing was chosen.

### 2.2 Solar cells

In a second step, n-type solar cells based on the high-efficiency structure used by Benick *et al.* [3] featuring the newly developed rear passivation and contact scheme (Fig. 1 and Fig. 2) were prepared. (100) n-Fz silicon wafers with a thickness of 230 µm were used. The cells (2×2 cm$^2$) feature a front surface with inverted pyramids and evaporated Al/Ti/Pd/Ag front contacts defined by photolithography which are thickened by electroplating. A $BBr_3$ diffusion at 890°C followed by a drive-in oxidation at 1050°C results in a homogeneous boron emitter with a sheet resistance of 140 Ω/sq. The cells do not feature an additional front surface diffusion for the formation of selective emitter regions. The front side boron emitter was passivated by 10 nm of $Al_2O_3$ deposited by plasma assisted atomic layer deposition (PA-ALD) followed by a $SiN_x$ layer as antireflection coating [6]. The rear side of the cell was processed as shown in Fig. 1. The *PassDop* layer on the basis of amorphous silicon carbide is deposited onto the whole rear surface followed by the laser process (analogous to the process applied to the lifetime samples) which

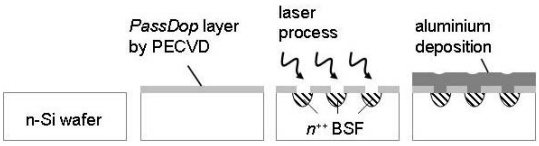


*Fig. 1: Schematic of the process sequence for the rear passivation and contacting of high-efficiency n-type silicon solar cells.*

simultaneously opens the rear dielectric films (variation of point spacing $L_p$=600−900 µm) and leads to a local $n^+$ region beneath the contact points. No subsequent cleaning or etching step is needed after the laser step. Subsequently, a 2 µm thick aluminium layer was evaporated on top by an e-gun process. The cells were then annealed at 350°C for 15 min to decrease the front contact resistance and to anneal the surface defects due to e-gun front and rear metallization. Finally the front contacts were thickened by Ag electroplating.

## 3 RESULTS

### 3.1 Lifetime samples

The calculation of the SRVs $S$ from the lifetime data of the symmetrically processed samples was done using the relation

$$\frac{1}{\tau_{eff}} = \frac{1}{\tau_{bulk}} + \frac{2S}{W}, \qquad (1)$$

with $W$ referring to the thickness of the samples. For $\tau_{bulk}$ the intrinsic lifetime limit determined by the model of Kerr *et al.* was applied, resulting in $\tau_{bulk}$=4500 µs for n-type 1 Ωcm silicon material (at $\Delta n$=5×10$^{14}$ cm$^{-3}$). Considering the analytical model proposed by Fischer for the calculation of an effective SRV at the contact points ($S_{cont}$) [7]

$$S_{eff} = \frac{D_h}{W}\left[\frac{L_p}{2W\sqrt{\pi f}}\arctan\left(\frac{2W}{L_p}\sqrt{\frac{\pi}{f}}\right) - \exp\left(-\frac{W}{L_p}\right) + \frac{D_h}{fWS_{cont}}\right]^{-1} + \frac{S_{pass}}{1-f}, \qquad (2)$$

the extracted SRVs before and after laser processing turn out to refer directly to $S_{pass}$ and $S_{eff}$, respectively. $D_h$ is the

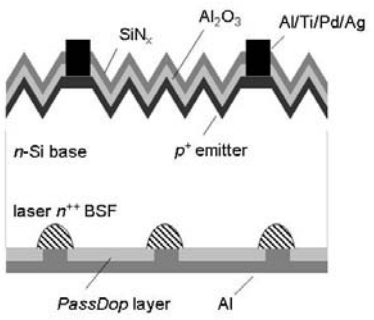


*Fig. 2: High-efficiency PERL structure with industrial feasible local rear BSF by laser doping. The dopants are provided by the PassDop layer stack during the laser contacting process prior to the rear aluminium evaporation.*

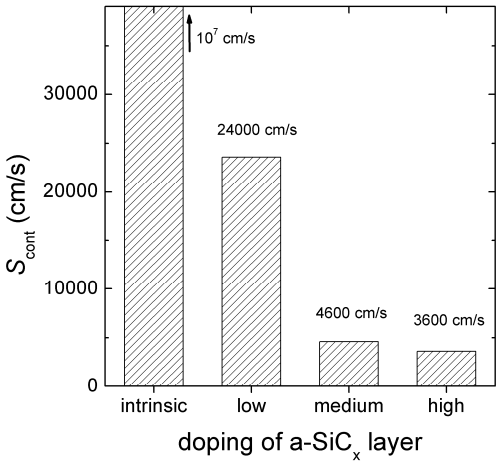


*Fig. 3: Dependence of the effective surface recombination velocity at the laser points $S_{cont}$ on the amount of phosphorus incorporated in the amorphous silicon carbide layer for a defined laser power. [8]*

diffusivity of the holes, $L_p$ is the spacing between the contact points and $f$ is the fraction of the laser affected surface. Note that in this respect the calculated $S_{cont}$ values are supposed to be slightly lower as compared to those encountered at solar cell level since a metal coverage additionally increases the recombination at the very surface of the contact points.

Fig. 3 shows the impact of the amount of dopant atoms available in the amorphous silicon carbide layer. In the case of an intrinsic film, formula (2) results in values for $S_{cont}$ indicating completely depassivated surfaces (here characterized by 10$^7$ cm/s according to the thermal velocity of charge carriers). With increasing doping density, $S_{cont}$ is effectively reduced to values below 4000 cm/s. This result points to a gentle, non-destructive laser doping process and an efficient local back surface field (LBSF) underneath the laser points.

### 3.2 Solar cells

The electrical performance of the *PassDop* approach is directly reflected by the open-circuit voltage $V_{oc}$ of the cells and the quality of the rear contact is directly linked to the fill factor *FF*.

The one-sun parameters of the fabricated n-type solar cells measured on an aperture area of 4 cm$^2$ are summarized in Table I. The best cell exhibits an open-circuit voltage ($V_{oc}$) of 701 mV, a short-circuit current ($J_{sc}$) of 39.8 mA/cm$^2$ and a fill factor (*FF*) of 80.1 % resulting in a solar cell efficiency of 22.4 %. The solar cell batch

*Table I: One-sun parameters of high-efficiency PERL n-type structures (aperture area of 4 cm$^2$) featuring an industrially feasible rear passivation and contacting scheme (PassDop).*

| | $V_{oc}$ (mV) | $J_{sc}$ (mA/cm$^2$) | *FF* (%) | $\eta$ (%) |
|---|---|---|---|---|
| average (76 cells)[a] | 698±3 | 40.1±0.2 | 79.3±0.8 | 22.2±0.2 |
| best cell[b] | 701 | 39.8 | 80.1 | 22.4 |

[a] internal measurements
[b] confirmed by Fraunhofer ISE CalLab

shows impressively the very high process stability resulting in an average $V_{oc}$ of 698 mV and a *FF* of 79.3 % for 76 processed solar cells. The elevated $V_{oc}$ in combination with a good *FF* for this industrially feasible rear side approach proves the very high performance of the applied rear passivation and contacting scheme. An effective suppression of carrier recombination at the rear side is proven by an excellent internal quantum efficiency (IQE) in the wavelength region between 900-1200 nm (Fig. 4). Additionally the *PassDop* layer acts as a reasonable rear reflector with effective internal reflection values of (93±1) % including the metallization points.

## 4 DISCUSSION

Of special interest is the performance of the laser induced local $n^+$ BSF and its influence on the cell parameters. Again, the most valuable quantity for the characterization of the local high-low junction is $S_{cont}$ which directly quantifies its electrical impact. An approximation of $S_{cont}$ can be performed departing from the one diode equation

$$V_{oc} = \frac{kT}{q} \ln\left(\frac{J_{sc}}{J_{0,total}} + 1\right). \qquad (3)$$

Using this relation, the total saturation current of the best cell $J_{0,total}=J_{0e}+J_{0b}$ results in 56 fA/cm$^2$. Assuming a very well passivated front surface and a value of 30 fA/cm$^2$ for the emitter saturation current $J_{0e}$ (including the metal contact areas) as proposed by Benick *et al.* for an equal cell structure [3] the base saturation current of our cell was determined to be 26 fA/cm$^2$. Assuming a bulk diffusion length of 0.23 cm ($\tau_{bulk}$=4500 µs) an upper limit for $S_{eff}$ at the rear side of the cell can be calculated by

$$J_{0b} = \frac{qD_h n_i^2}{LN_D}\left[\frac{\left(S_{eff}L/D_h\right)+\tanh\left(W/L\right)}{1+\left(S_{eff}L/D_h\right)\tanh\left(W/L\right)}\right]. \qquad (4)$$

In this equation $q$ refers to the elementary charge, $D_h$ is the diffusivity of the holes, $n_i$ is the intrinsic carrier concentration and $N_D$ is the doping concentration of the bulk. The calculated $S_{eff}$ amounts to 6 cm/s. Using a value of $S_{pass}$=3 cm/s as determined on the lifetime samples for equally passivated surfaces and 40 µm for the visible diameter of the laser points, equation (2) yields a $S_{cont}$ of approximately 2000 cm/s which is in the same order as the value determined previously at the lifetime level. For comparison, Benick *et al.* report on a $S_{cont}$ of 55 cm/s for their deep diffused phosphorus LBSF [3]. However, considering the simplicity of the process, the achieved quality of the laser-induced BSF is very promising for the industrial implementation of a $n^+$ LBSF.

## 5 CONCLUSION

Very high $V_{oc}$ of 701 mV and *FF* of 80.1% were achieved on n-type PERL solar cells featuring a newly developed rear passivation and contacting scheme based on phosphorus doped amorphous silicon carbide (*PassDop*). During a laser process the latter serves as both, passivation layer and doping source. The results show impressively the high potential of this rear concept for industrial n-type solar cells. Compared to the laboratory high-efficiency rear side for this cell structure comprising an additional diffusion step for the local $n^+$ LBSF and several steps of photolithography resulting in $V_{oc}$´s up to 703 mV, the presented approach is simple and industrially feasible, however maintaining a very high level of cell performance.

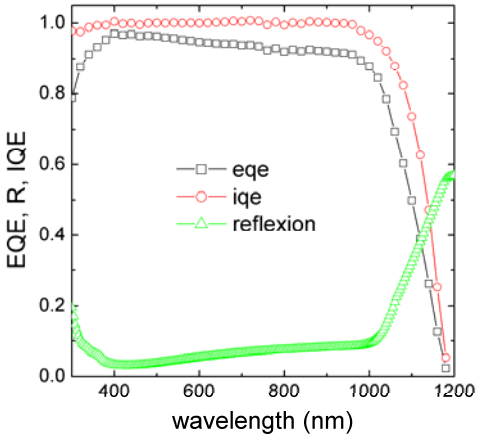


*Fig. 4: Reflectance (R), external and internal quantum efficiency (EQE/IQE) of a high-efficiency n-type cell with PassDop rear side scheme. [8]*

## 6 ACKNOWLEDGMENT

The authors would like to thank S. Seitz, A. Leimenstoll, F. Schätzle, N. König and I. Druschke for processing and E. Schäffer for measuring of the solar cells.

## 7 REFERENCES

[1] D. De Ceuster, P. Cousins, D. Rose, D. Vicente, P. Tipones and W. Mulligan, Proceedings of the 22nd European Photovoltaic Solar Energy Conference, Milan, Italy (2007) 816.

[2] M.A. Green, K. Emery, Y. Hishikawa and W. Warta, Progress in Photovoltaics: Research and Applications 17 (2009) 320.

[3] J. Benick, B. Hoex, M.C.M. van de Sanden, W.M.M. Kessels, O. Schultz and S.W. Glunz Applied Physics Letters 92 (2008) 253504/1.

[4] J. Benick, B. Hoex, G. Dingemans, A. Richter, M. Hermle and S.W. Glunz Proceedings of the 24th European Photovoltaic Solar Energy Conference, Hamburg, Germany (2009) 863.

[5] R.A. Sinton and A. Cuevas, Applied Physics Letters 69 (1996) 2510.

[6] J. Schmidt, A. Merkle, R. Bock, P.P. Altermatt, A. Cuevas, N.-P. Harder, B. Hoex, R. van de Sanden, E. Kessels and R. Brendel, Proceedings of the 23rd European Photovoltaic Solar Energy Conference, Valencia, Spain (2008) in print.

[7] B. Fischer, Loss analysis of crystalline silicon solar cells using photoconductance and quantum efficiency measurements, Dissertation, Universität Konstanz, Konstanz, 2003.

[8] D. Suwito, U. Jäger, J. Benick, S. Janz, M. Hermle and S. Glunz, IEEE Transactions on Electron Devices 57 (2010) 2032.